



Numerical study of wave breaking for monochromatic and grouping waves in deep water

T. A. Pullen⁽¹⁾, K. She⁽²⁾, J. Morfett

*School of the Environment, Cockcroft Building, University of Brighton,
Lewes Rd, Brighton, BN2 4GJ, UK*

Email: ⁽¹⁾i.a.pullen@bton.ac.uk ⁽²⁾k.m.she@bton.ac.uk

Abstract

A fully nonlinear 2-dimensional numerical wave flume, based on the boundary integral equation method, has been developed. Waves are generated by a hinged paddle wave maker at one end of the flume and a sponge type wave absorber at the other end. A fourth order Taylor expansion technique is used for the time stepping of the free surface. Simple monochromatic waves have been generated and very good agreements are found when compared with Stokes wave profiles. The wave flume is used to study deep water wave breaking due to large periodic displacements of the wave paddle. Wave breaking as a result of energy focusing a group of waves of different frequencies and heights, is also studied. For each breaking event, breaking wave parameters such as the wave steepness, breaking height, particle velocities and accelerations are examined in detail. There does not appear to be a definable correlation between the point of breaking, the wave steepness, or the particle velocities. The maximum downward (vertical) and forward (horizontal) accelerations at breaking are found to be independent of the initial conditions, with constant values of g and $1.56g$, respectively; and where g is the acceleration due to gravity. It has been proposed (Philips¹) that particle accelerations could be used as a criterion for wave breaking. Positive verification of this was first provided in an earlier study by the authors She et al², which used spatially periodic boundary conditions. Both studies support Philips' conjecture, and suggest that the point of breaking is when the maximum vertical and horizontal accelerations are at g & $1.56g$.



1 Introduction

Wave breaking represents the most extreme surface sea conditions. The accuracy of predicting wave breaking directly affects the accuracy of our prediction of the extreme wave forces on offshore and coastal structures. It also affects our ability to accurately predict coastal processes such as sediment transport. Because of its engineering significance, wave breaking has been a subject of great interest over the last two decades. Amongst some notable works are those of Longuet-Higgins & Cokelet³, Dold & Peregrine⁴, New et al⁵, Grilli & Subramanya⁶, and Lin & Liu⁷.

Experimental studies of wave breaking can be expensive and difficult to implement. Despite the introduction of highly advanced measuring techniques in recent years, accurate measurements of full field particle accelerations in a breaking wave have yet to be achieved. Recent studies of wave breaking in 3D sea conditions by She et al⁸ postulated that the examination of acceleration in breaking waves may hold the key in reaching a universally applicable breaking criterion, which is supported by the numerical study of She et al². The present study further examines the accelerations of breaking waves through a numerical wave flume.

2 The Numerical Wave Flume

2.1 Governing Equations

The numerical wave flume is shown in Figure 1. The fluid boundary(Γ) is represented by discretised computational nodes, and consists of the free surface (Γ_{FS} & Γ_{NB}), a solid boundary(Γ_{SB}), and a hinged paddle wave maker(Γ_P). The surfaces Γ_{SB} and Γ_P are assumed to be impermeable. Let the fluid motion be 2-dimensional, incompressible, inviscid and irrotational, then it may be described by the complex velocity potential $\Phi = (\phi, \psi)$, such that

$$u - iv = \frac{d\Phi}{dZ} \quad (1)$$

which satisfies the nonlinear free surface kinematic boundary condition, and where $Z=(x, y)$. Making use of Cauchy's theorem, we have

$$\oint_{\Gamma} \frac{\Phi(Z) - \Phi(Z_n)}{Z - Z_n} dZ = 0 \quad (2)$$

The nonlinear dynamic free surface boundary condition is satisfied by Bernoulli's equation,

$$\frac{d\phi}{dt} = -\frac{P_a}{\rho} - gy + \frac{1}{2}(u^2 + v^2) \quad \text{on } (\Gamma_{FS} \text{ \& } \Gamma_{NB}) \quad (3)$$

where P_a , ρ and g , are the atmospheric pressure, the fluid density and the acceleration due to gravity, respectively. Along the paddle surface we have the stream function,

$$\psi = \frac{1}{2}r^2\omega \quad \text{on } (\Gamma_P) \quad (4)$$

where r is the distance between O_P and a fluid particle on the paddle surface, and ω is the paddle's angular velocity. Finally, on the solid boundary we have,

$$\psi = 0 \quad \text{on } (\Gamma_{SB}). \quad (5)$$

Equations 1 to 5 form the basis for the numerical model, and are solved by the boundary integral equation method. Further details on the solution of these equations, may be found in the earlier work by She et al⁹.

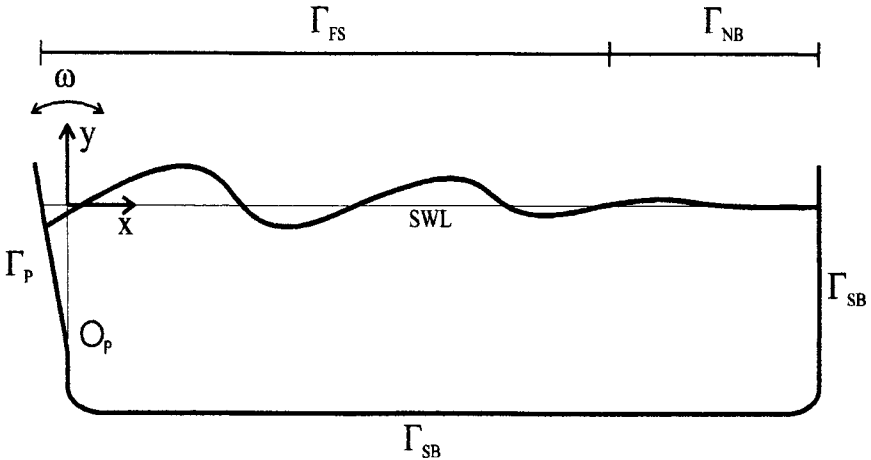


Figure 1: The numerical wave flume.

2.2 Numerical implementation

The method takes advantage of the mixed Eulerian-Lagrangian technique of Longuet-Higgins & Cokelet³. The velocity potential on the free surface is set to zero at time $t=0$. That is, the fluid surface is at the still water level (SWL), and the paddle is in the upright position. We are therefore able to solve for the initial condition, and then determine the higher Eulerian and Lagrangian derivatives. An

226 *Coastal Engineering and Marina Developments*

algorithm similar to that of Dold & Peregrine⁴ is used, where each step provides the necessary information for solving the next. We solve up to the fourth derivatives, and use a fourth order Taylor expansion for time stepping the free surface.

The only input into the model, is the wave paddle angular velocity ω , where

$$\omega(t) = \gamma \sum_{i=1}^N \omega_i \cos(2\pi f_i t + \varphi_i) \quad (6)$$

and ω_i , f_i and φ_i , are the input paddle angular velocity, wave frequency and phase angle, respectively, and N are the number of waves to be input. The paddle motion is a superposition of a number of sine waves. To achieve a required wave height for a given frequency, a transfer function is used to determine the value of ω_i and φ_i . More discussion on this can be found in section (4) below. γ is a 'cold start' function, which allows the wave paddle to be gradually brought up to speed, and is given by,

$$\gamma = 1 - \exp\left(\frac{-C}{T} t\right) \quad (7)$$

where $C = 6$, and T is a prescribed time delay, usually 1 s.

To counter the problem of wave reflection, we suppress the free surface velocities u & v , by the wave absorption function,

$$\alpha = \exp\left(-\frac{1}{2}(x - x_{NB})^3\right) \quad \text{on } (\Gamma_{NB}) \quad (8)$$

where x_{NB} is the start of Γ_{NB} , and Γ_{NB} is generally 25~30% of the total length of the wave flume.

2.3 Numerical performance

A comparison of the wave profiles, velocity potentials, stream functions and surface velocities, of monochromatic waves generated in the flume, have been made. These have shown a very good agreement with Stokes waves generated by the nonlinear equations of Schwartz¹⁰. For further details on the general performance of the model, the reader is referred to the earlier work by She et al⁹.

3 Generation of breaking waves

There were two approaches to generating breaking waves in this study. Monochromatic waves were generated with an input frequency of 1 Hz. A number of runs were performed, gradually increasing the amplitude of the paddle movement.

Multiple frequency waves were generated, and wave breaking was achieved as a result of energy focusing. Component wave heights are determined using the same function as that used by Skyner et al¹¹ and She et al⁸, given by

$$H_i = H_0(1 + f_i) \exp \left[- \left(\frac{f_i - f_1}{f_0} \right)^S \right] \quad (9)$$

where $f_0 = 0.55$ Hz, $f_1 = 0.85$ Hz, $S = 16$ and H_0 is a constant. The general variation of H/H_0 as a function of f_i is shown in Fig 2. For the purpose of this study $f_i = 0.6\text{--}1.4$ Hz.

A breaking wave height H_B is then specified for a given spatial and temporal focusing point, such that $H_B = \Sigma H_i$. Eqn (9) has been shown to generate very good 2-dimensional breakers. However, the only variable in eqn (9) is the paddle frequency, but we use eqn (6) to generate the wave group. We therefore require a relationship between the height and the variables in eqn (6), which we present in the next section.

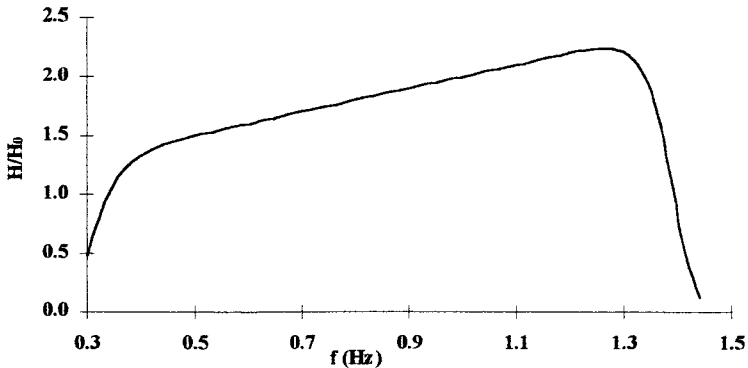


Figure 2: Wave height as a function of frequency.

4 Wave Flume Calibrations

To relate the wave height to the input parameters for eqn (6), it was necessary to perform a large number of wave runs for monochromatic waves. To do this the

228 *Coastal Engineering and Marina Developments*

paddle frequency was chosen in the range $f = 0.6\text{--}1.4$ Hz, and for each value of f the paddle angular velocity was varied, such that $\omega = 0.005\text{--}0.200$ rad s^{-1} . Numerical wave gauges were set up to allow the wave elevations to be recorded as a function of time. From the wave gauge records it was possible to determine the time averaged wave heights and wavelengths, taken after a steady wave train had fully developed.

For each value of f , a very good agreement to a least squares quadratic fit was found between ω and H , in the form

$$\omega = a_f + b_f H + c_f H^2 \quad (10)$$

where a_f , b_f and c_f are the least squares coefficients for each frequency. Similarly, there is a relationship between H/L and ω , once again in the form

$$\frac{H}{L} = a_{f\omega} + b_{f\omega} \omega + c_{f\omega} \omega^2 \quad (11)$$

where $a_{f\omega}$, $b_{f\omega}$ and $c_{f\omega}$ are the coefficients for each frequency.

The coefficients of eqns (10 & 11) are then fitted to polynomial expressions, such that they cover all possible frequencies between 0.6 & 1.4 Hz. We then have two general functions, given by

$$\omega_i = A + B H_i + C H_i^2 \quad (12)$$

and,

$$\frac{H_i}{L_i} = D + E \omega_i + F \omega_i^2 \quad (13)$$

where A , B , C , D , E and F are 6th order polynomial functions of f_i . Since H_i and f_i are prescribed, the solutions of eqns (12 & 13) provide us with the values for ω_i and L_i , and from L_i we can find $k_i = 2\pi/L_i$. For the focusing wave study, the phase angle of each front is given by

$$\varphi_i = k_i x_{FP} - 2\pi f_i t_{FP} \quad (14)$$

where x_{FP} and t_{FP} are the spatial and temporal focusing points, respectively.

The use of 6th order polynomials in eqns (12 & 13) may seem excessive. However, when the computed and actual values for the heights and wavelengths are compared, the averaged errors are 0.74% and 0.36%, respectively.

Moreover, when monochromatic waves were focused using these equations, they were found to behave as predicted, sometimes arriving exactly as prescribed. Figure 3 shows eqn (12) plotted for a frequency of 1 Hz, along with the original height and paddle angular velocity data for a 1 Hz wave.

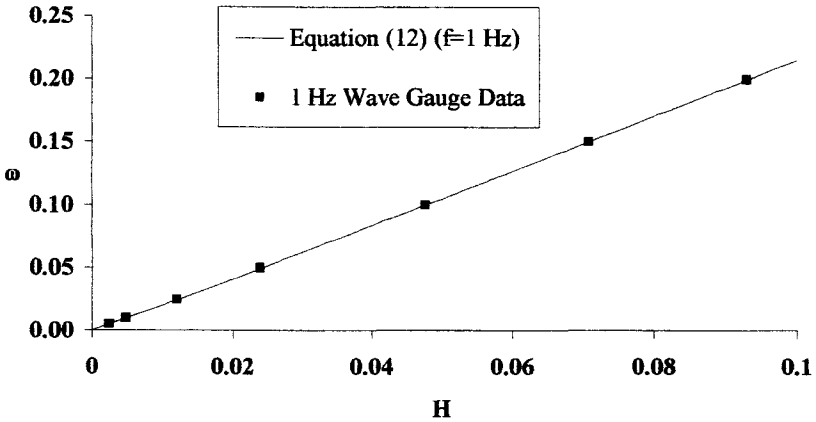


Figure 3: The relationship between H & ω for a paddle frequency $f=1$ Hz

5 Results and discussion

Figure 4 shows a fully developed monochromatic wave train at time $t=12$ s. There is a high repeatability of the wave profiles, and an examination of the wave gauge records indicates that the wave reflection is very small. Wave height variations are usually less than 1%.

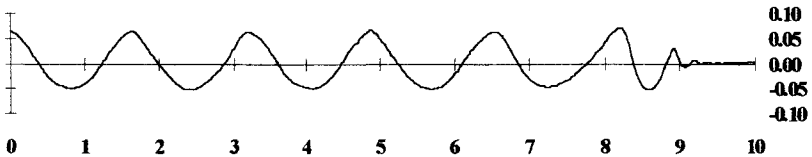


Figure 4: A fully developed monochromatic wave train.

Wave breaking is taken to be the point when the front face of the wave becomes vertical (see Griffiths et al¹²). We investigate the classical definition of the wave total steepness. The crest rear (RS) and crest front (FS) steepness are also investigated, where these are either side of the crest and above the still water level. Figure 5 shows the steepness for the monochromatic and grouping waves, as a function of the breaking wave height. Wave steepness is a traditional criterion for defining the point of breaking. There does not appear to be a clearly



defined correlation between the breaking wave height and the steepness parameters, supporting the earlier work of the authors She et al².

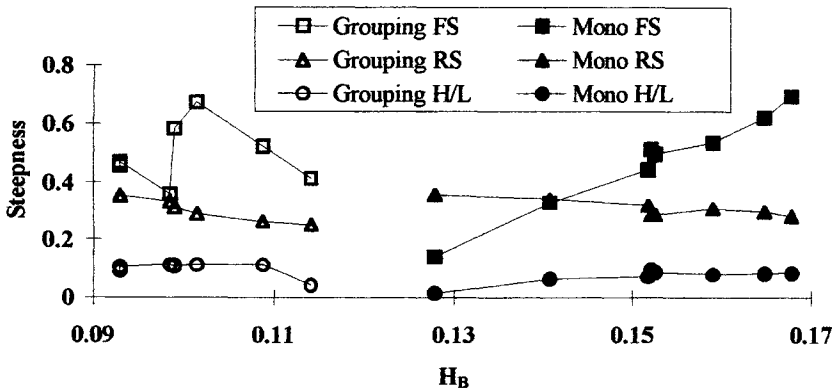


Figure 5: Wave steepness at breaking.

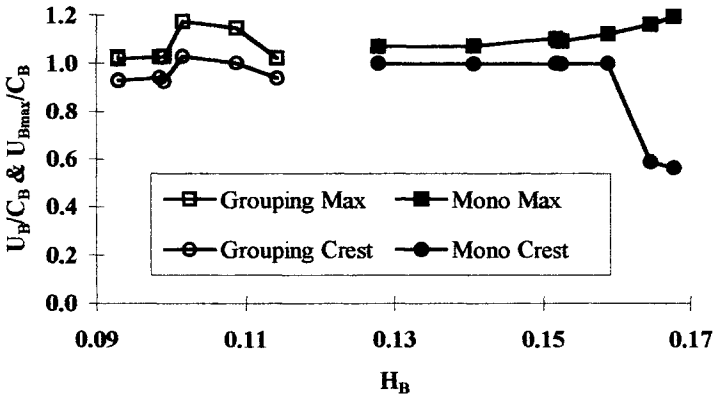


Figure 6: Crest and maximum particle velocities at breaking.

Griffiths et al¹² suggested that a velocity based breaking criterion may be applicable. Further study by She et al⁸ indicated the possibility of using the maximum velocity in the crest as a breaking criterion, but suggested that the acceleration is likely to be a better parameter for this purpose. Figure 6 shows the relationship between the breaking velocities and the breaker height. There does not appear to be a correlation between the crest particle velocities (U_B), and the wave celerity, at the point of breaking. The maximum velocities are U_{Bmax} , which are the front face velocities at the point of breaking, this has been reported

by Griffiths et al¹² and She et al⁸. When this is compared with the wave celerity at breaking (C_B), it is apparent that the two velocities are similar, but with no obvious relationship.

Phillips¹ was the first to suggest that the particle accelerations could be used as a criterion for wave breaking. The results of the analysis of the particle accelerations are shown in figure 7. The maximum vertical accelerations are towards the top of the front face of the breaker, and are very close to $1g$, suggesting that the water is in free fall. The maximum horizontal accelerations are in the front face of the breaker, and below the point of maximum vertical acceleration. The values of the horizontal acceleration are found to be approximately constant at a value $1.56g$. In comparison with other parameters, the particle accelerations are best and most simply defined in relation to the breaker heights, supporting the earlier work by the authors She et al².

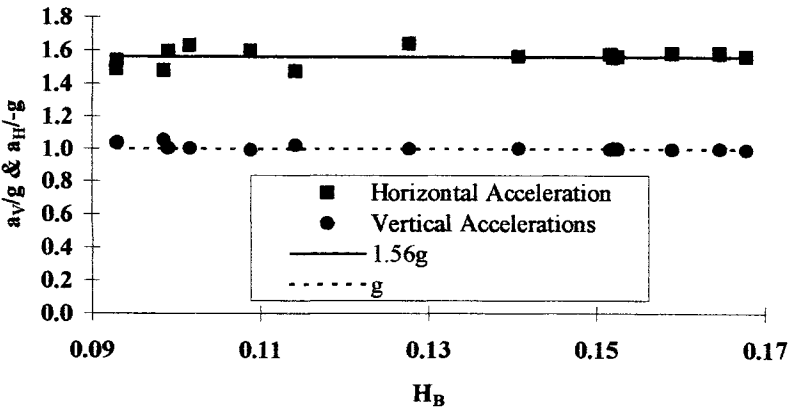


Figure 7: A comparison of the accelerations and the heights at breaking.

6 Conclusion

A fully nonlinear numerical wave flume has been developed. Wave breaking has been studied for monochromatic and grouping waves. The wave steepness, particle velocities and accelerations have been examined for a range of breaking waves. It has been shown that the particle accelerations are best suited for establishing a universally applicable breaking criterion. The limited case studies carried out so far, shows that the point of breaking is when the maximum horizontal and vertical (downward) particle accelerations reach values of $1.56g$ and g , respectively. Further work is underway to investigate breaking under transitional and shallow water conditions.



References

1. Phillips, O. M. The equilibrium range in the spectrum of wind generated waves. *J. Fluid. Mech.* **4**, pp. 785-790. 1958.
2. She, K. Pullen, T.A. Morfett, J. Numerical study of breaking wave parameters. *Proc. Of the 3rd Int. Conf. On Hydro-Science and Engineering*, eds. K.P. Holz, W. Bechteler, S.S.Y. Wang, M. Kawahara, ICHE, Cottbus, Germany. 1998.
3. Longuet-Higgins, M.S. Cokelet, E.D. The deformation of steep surface waves on water. I. A numerical method of computation. *Proc. R. Soc. Lond.* **350 A1-26**. 1976.
4. Dold, J.W. Peregrine, D.H. An efficient boundary integral method for steep unsteady water waves. *Numerical methods for Fluid Dynamics II*, Clarendon Press. pp. 671-679. 1985.
5. New, A.L. McIver, P. Peregrine, D.H. Computations of overturning waves. *J. Fluid. Mech.* **150**. pp 233-251. 1985.
6. Grilli, S.T. Subramanya, R. Numerical modelling of wave breaking induced by fixed or moving boundaries. *Computational Mech.* **17**. pp 374-391. 1996
7. Lin, P. Liu, P.L-F. A numerical study of breaking waves in the surf zone. *J. Fluid. Mech.* **359**. pp 239-264. 1998.
8. She, K. Greated, C.A. Easson, W.J. Experimental study of three-dimensional breaking wave kinematics. *App. Ocean. Res.* **19 Nos 5-6** pp 329-343. 1997.
9. She, K. Greated, C.A. Easson, W.J. Development of a two dimensional numerical wave tank. *Proc. 2nd Int. Offshore and Polar Eng. Conf.*, San Francisco, USA. 1992.
10. Schwartz, L.W. Computer extension and analytic continuation of Stokes' expansion for gravity waves. *J. Fluid. Mech.* **62 Part 3** pp 553-578. 1974
11. Skyner, D.J. Gray, C. Greated, C.A. A comparison of time stepping numerical predictions with whole field flow measurement in breaking waves. *Water wave kinematics*. Kluwer Academic Publishers, Dordrecht. pp 491-508. 1990.
12. Griffiths, M.W. Easson, W.J. Greated, C.A. Measured internal kinematics for shoaling waves with theoretical comparisons. *J. Waterway, Port, Coastal, and Ocean Eng.* **118 No 3** pp 280-299. 1992